

# Ultra-low density InAs quantum dots

© V.G. Dubrovskii<sup>†\*</sup>, G.E. Cirlin<sup>\*+</sup>, P.A. Brunkov<sup>+</sup>, U. Perimetti<sup>\*</sup>, N. Akopyan<sup>\*</sup>

\* St. Petersburg Academic University Russian Academy of Sciences,  
194021 St. Petersburg, Russia

<sup>2</sup> Ioffe Physical Technical Institute Russian Academy of Sciences,  
194021 St. Petersburg, Russia

<sup>\*</sup> Quantum Transport, Kavli Institute of Nanoscience, Delft University of Technology,  
2628CJ Delft, The Netherlands

(Получена 18 февраля 2013 г. Принята к печати 25 февраля 2013 г.)

We show that InAs quantum dots (QDs) can be grown by molecular beam epitaxy (MBE) with an ultralow density of  $\sim 10^7 \text{ cm}^{-2}$  without any preliminary or post-growth surface treatment. The strain-induced QD formation proceeds via the standard Stranski–Krastanow mechanism, where the InAs coverage is decreased to 1.3–1.5 monolayers (MLs). By using off-cut GaAs(100) substrates, we facilitate the island nucleation in this subcritical coverage range without any growth interruption. The QD density dependences on the InAs coverage are studied by photoluminescence, atomic force microscopy, transmission electron microscopy, and are well reproduced by the universal double exponential shapes. This method enables the fabrication of InAs QDs with controllable density in the range  $10^7$ – $10^8 \text{ cm}^{-2}$ , exhibiting bright photoluminescence.

## 1. Introduction

Interest in low density ( $\sim 10^8 \text{ cm}^{-2}$  and lower) In(Ga)As/GaAs quantum dots (QDs) ranges from fundamental physics of single semiconductor zero-dimensional nanostructures to a variety of promising applications in QD-based single photonic devices, where the avoidance of crosstalk is essential [1]. However, a random character of the stress-induced formation of the Stranski–Krastanow QDs in lattice-mismatched systems such as InAs/GaAs (lattice mismatch  $\approx 7\%$ ) [2,3] makes it difficult to considerably reduce the surface density  $N$ . Several methods have been proposed to overcome this difficulty, e.g., droplet phase epitaxy [4,5], MBE growth on GaAs substrates with an intentional temperature gradient [6], growth on lithographically defined nanoholes [7], or lateral positioning of QDs using a buried stressor [8]. More sophisticated methods can also be applied, such as top-down etching of quantum well heterostructures into quantum dot micropillars [9], and bottom-up vapor-liquid-solid growth of axial nanowire heterostructures [10]. Most of these techniques enable a good position control, but necessarily require advanced lithography or post-growth patterning. In the self-induced approach, low density islands can be obtained only by applying very low deposition rates [11,12], where going below  $10^8 \text{ cm}^{-2}$  remains challenging.

In this work, we utilize the self-induced approach in the so-called subcritical coverage range [12], i.e. below the critical thickness  $H_c$  for the  $2D$ – $3D$  growth transformation under the material influx ( $H_c \approx 1.7 \text{ MLs}$  in the InAs/GaAs system [13]). As was noticed in a number of earlier works (see, e.g., Ref. [14–16]), while the reflection high energy electron diffraction (RHEED) pattern remains streaky below 1.7 MLs, 3D islands can still form at a low nucleation rate. This was further developed in Refs. [17,18] by showing that InAs QDs can form on singular GaAs(100) substrates at

1.5–1.6 MLs coverage upon a certain exposition to arsenic flux. By applying classical nucleation theory to the stress-driven growth process [17–20], it has been argued that that  $H_c$  has a kinetic origin (the maximum wetting layer thickness relating to the maximum nucleation rate), while the wetting layer metastability actually starts from a lower equilibrium thickness  $H_{\text{eq}} \approx 1 \text{ ML}$ . The island formation was therefore possible between  $H_{\text{eq}}$  and  $H_c$ . These subcritical InAs QDs were then grown by MBE on off-cut substrates, exhibiting a bright photoluminescence (PL) [21]. Here, we study the formation of subcritical InAs QDs in more detail, and quantize their densities by different characterization techniques and theoretical modeling.

## 2. Experimental

Growth experiments were carried out in an EP1203 MBE setup equipped with a RHEED system. QD layers were grown on singular and cut-off GaAs(100) substrates with different misorientation angles ( $3$ – $7^\circ$ ) at a substrate temperature of  $485^\circ\text{C}$  and InAs deposition rate  $V = 0.05 \text{ ML/s}$ , with no intentional exposition to arsenic flux after the growth. The deposition thickness  $H$  was varied from 1.2 to 2 MLs. Some samples were remained uncovered for atomic force microscopy (AFM) measurements, other were confined from both sides by the AlGaAs/GaAs superlattices for PL measurements. These samples were also characterized by transmission electron microscopy (TEM). *In situ* RHEED diagnostics did not reveal the transformation from streaky to spotty below 1.65–1.75 MLs for all samples, which confirms the value of critical thickness of  $\sim 1.7 \text{ MLs}$ .

Besides AFM characterization, the surface density of InAs islands was obtained by looking at their PL spectra. For the low density samples with 1.3 and 1.4 ML of InAs deposited, it was possible to estimate the density by simply shining the laser light over an extended area of the sample and imaging the PL on a CCD camera (Figs 1, *a-c*). The

<sup>†</sup> E-mail: dubrovskii@mail.ioffe.ru

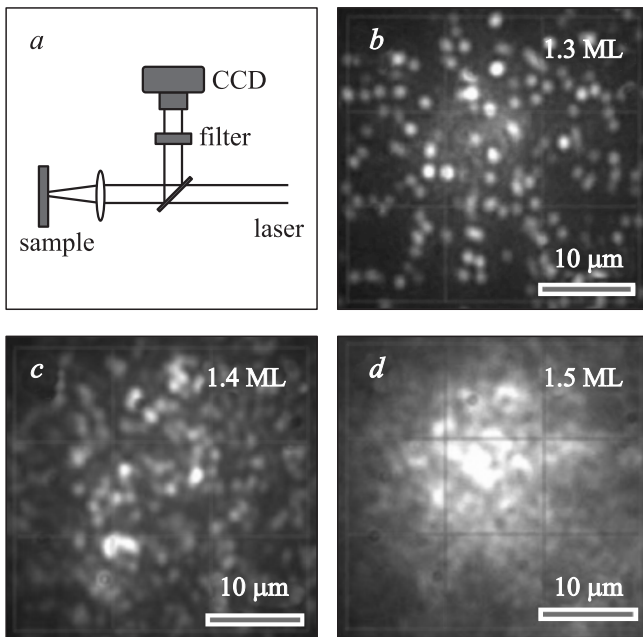


**Figure 1.** Schematics of PL measurements (a) and PL images of 1.3 (b), 1.4 (c) and 1.5 (d) ML InAs QDs on  $5^\circ$  off-cut GaAs(100) substrates.

scale of the image was calibrated based on lithographically defined markers on the sample surface. The sample with 1.5 ML of InAs (Fig. 1, d) showed too high density of QDs that could not be determined by simple imaging but required some spectroscopic measurements. The density on 1.5 ML samples was therefore counted in the following way. A region of a sample was scanned in discrete steps and a spectrum was recorded at each point. In this way the PL intensity maps were obtained at different wavelengths. We let a Matlab script find the location of peaks on each map in order to have a list of different optical transitions originating from different dots. To determine the number of islands, it was then necessary to divide these transitions in groups that belong to the same dot. Different transitions were attributed to the same dot if they were located within a certain distance  $d$  and if their wavelengths differ by less than  $\Delta\lambda$ . The choice of  $d$  and  $\Delta\lambda$  was made based on the spatial resolution of the system and the confinement energy of QDs.

### 3. Results and discussion

From the analysis of both PL and structural characterization data, it has been found that the QD density rapidly decreases toward smaller  $H$  at a given cut-off angle; and usually decreases with decreasing the cut-off angle at a given coverage. Consistent with our previous results [17], no QDs were found on singular substrates below 1.5 ML coverage, and no QDs were seen in 1.2 ML samples regardless of the cut-off angle. In particular, Fig. 2 shows typical AFM images of subcritical InAs QDs in 1.3 (a) and 1.4 (b)  $5^\circ$  off-cut samples; and a typical TEM image of supercritical 2 ML sample (c).

of uncovered 1.3 and 1.4 MLs samples, and a TEM image of the capped 2 ML sample; all grown on the  $5^\circ$  off-cut GaAs substrates. It is seen on Fig. 2, b that subcritical QDs tend to decorate the surface steps where the nucleation barrier is lowered with respect to on-the-terrace case. The data are summarized in Table. AFM and PL data for the subcritical samples were consistent, showing that the vast majority of QDs participate in optical recombination.

Density versus coverage on  $5^\circ$  cut-off substrates

Coverage $H$ (MLs)	Surface density $N$ ( $\text{cm}^{-2}$ )
1.3	$1.2 \cdot 10^7 \pm 6\%$
1.4	$2.5 \cdot 10^7 \pm 6\%$
1.5	$3 \cdot 10^8 \pm 30\%$
2	$4 \cdot 10^{10} \pm 10\%$

To understand these data, we use the model of stress-driven islanding of Refs [17,18,20], adapted to the case of subcritical coverage without exposition. In brief, the driving force for 3D islanding is the relaxation of elastic stress in the islands that strongly depend on the aspect ratio [22,23]. However, this energetically favored relaxation is suppressed by the energetically costly processes of building the lateral facets and the work done against the wetting force. Therefore, islands can form only when  $H$  exceeds the equilibrium thickness  $H_{\text{eq}}$ , estimated at  $\sim 1$  ML [17], with the nucleation barrier  $F(H)$ . During the short-scale nucleation stage, islands are assumed as being of a fixed shape. In this case, the nucleation rate depends on

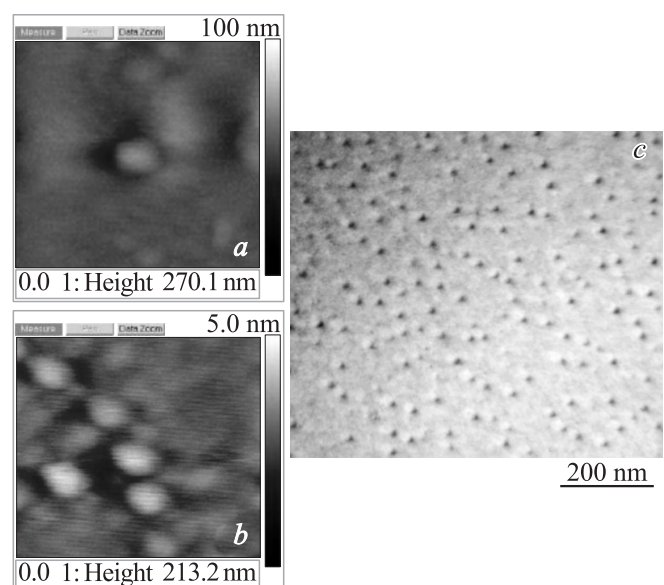


**Figure 2.** Typical AFM images of subcritical InAs QDs in 1.3 (a) and 1.4 (b)  $5^\circ$  off-cut samples; and a typical TEM image of supercritical 2 ML sample (c).

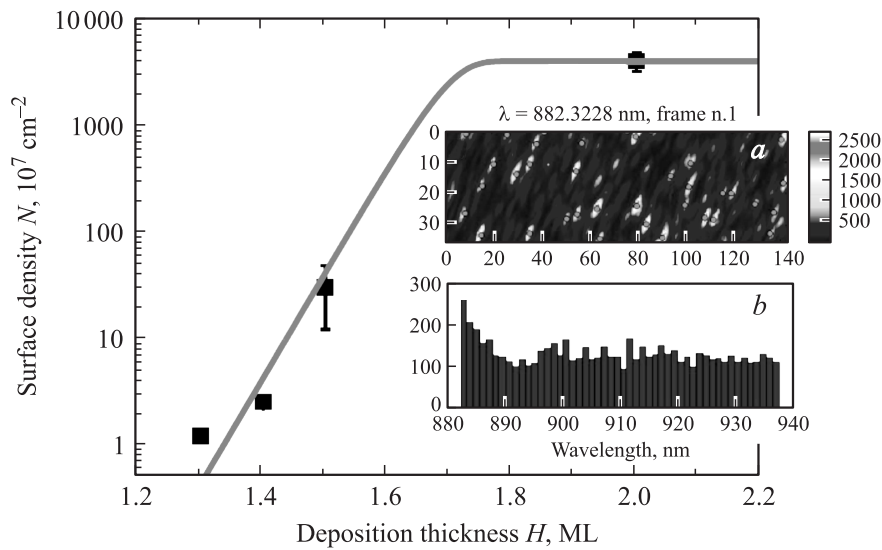


**Figure 3.** Experimental (symbols) and theoretical (line) dependences of the density of subcritical InAs QDs on  $5^\circ$  off-cut GaAs(100) substrates on the deposition thickness. The insert shows the PL map and QDs counts in the 1.5 ML sample.

time as [20]

$$I(t) = \frac{N_{\max}}{\Delta t} \exp \left[ \frac{t - t_c}{\Delta t} - \exp \left( \frac{t - t_c}{\Delta t} \right) \right], \quad (1)$$

where  $N_{\max}$  is the maximum surface density upon the completion of the nucleation stage,  $t_c$  is the time relating to the critical deposition thickness,  $\Delta t = (H_c - H_{\text{eq}})/(\Gamma V)$  is the characteristic nucleation time, and  $\Gamma$  is the large quantity that equals twice the nucleation barrier at the critical thickness. Integration of Eq. (1) over time yields the surface density, which can be presented as a function of coverage  $H = Vt$  in the form

$$N(H) = N_{\max} \left[ 1 - \exp \left( - \exp \left( \frac{\Gamma(H - H_c)}{H_c - H_{\text{eq}}} \right) \right) \right]. \quad (2)$$

We note that subcritical QDs at zero exposition relate to the left tail of this double-exponential distribution. In other words, these islands form well before the maximum of nucleation rate is reached, and would be almost invisible in the entire super-critical spectrum.

Experimental data in Fig. 3 are fitted by Eq. (2) with the known values of  $N_{\max} = 4 \cdot 10^{10} \text{ cm}^{-2}$ ,  $H_c = 1.7 \text{ ML}$  and  $H_{\text{eq}} = 1 \text{ ML}$ , at  $\Gamma = 16$ . It is seen that the fit is reasonable; a slightly off-line point at 1.3 ML is most probably explained by an unintentional exposure of the sample during re-growth. The estimated nucleation barrier allows one to deduce some important energetic and kinetic parameters of the system, which will be presented elsewhere.

To sum up, the described MBE procedure enables the fabrication of InAs QDs with ultralow and controllable density in the range  $10^7 - 10^8 \text{ cm}^{-2}$ . It has been shown that this becomes possible simply because the wetting layer metastability is much lower at the subcritical coverage, and islands nucleate at a lower rate. The use of off-cut GaAs

substrates is important to promote the nucleation at the surface steps. Theoretical model fits well the data and explains mechanism of subcritical islanding. Our results might be useful for synthesis of low density islands in other lattice mismatched systems, and for the controlled fabrication of InAs/GaAs QDs and other semiconductor islands for different applications. In particular, this method can be used to reduce the surface density of self-induced GaN islands on Si substrates that initiate the formation of highly-anisotropic nanowires at the follow-up growth stage [24].

**Acknowledgements:** This work was partially supported by the contracts with the Russian Ministry of Education and Science, grants of the Russian Foundation for Basic Research, and scientific programs of the Russian Academy of Sciences.

## References

- [1] *Single Semiconductor Quantum Dots*, ed. by P. Michler (Springer, Heidelberg, 2009).
- [2] L. Goldstein, F. Glas, J.Y. Marzin, M.N. Charasse, G. Le Roux. *Appl. Phys. Lett.*, **47**, 1099 (1985).
- [3] V.A. Shchukin, N.N. Ledentsov, D. Bimberg. *Epitaxy of Nanostructures* (Springer Verlag, N.Y., 2003).
- [4] J.S. Kim, N. Koguchi. *Appl. Phys. Lett.*, **85**, 5893 (2004).
- [5] B.L. Liang, Zh.M. Wang, J.H. Lee, K. Sablon, Yu.I. Mazur, G.J. Salamo. *Appl. Phys. Lett.*, **89**, 043 113 (2006).
- [6] P. Jin et al. *Nanotechnology*, **16**, 2775 (2005).
- [7] A. Huggenberger, S. Heckelmann, C. Schneider, S. Hofling, S. Reitzenstein, L. Worschech, M. Kamp, A. Forchel. *Appl. Phys. Lett.*, **98**, 131 104 (2011).
- [8] E. Stock, T. Warming, I. Ostapenko, S. Rodt, A. Schliwa, J.A. Tofflinger, A. Lochmann, A.I. Toropov, S.A. Moshchenko, D.V. Dmitriev, V.A. Haisler, D. Bimberg. *Appl. Phys. Lett.*, **100**, 093 111 (2012).

- [9] S. Reitzenstein, A. Forchel. *J. Phys. D: Appl. Phys.*, **43**, 033 001 (2010).
- [10] V.G. Dubrovskii, G.E. Cirlin, V.M. Ustinov. *Semiconductors*, **43**, 1539 (2009).
- [11] F. Zhan, S.S. Huang, Z.C. Niu, H.Q. Ni, Y.H. Xiong, Z.D. Fang, H.Y. Zhou, Y. Luo. *J. Nanosci. Nanotechnology*, **9**, 844 (2009).
- [12] A. Urbańczyk, R. Nötzel. *J. Cryst. Growth*, **341**, 24 (2012).
- [13] I. Mukhametzhanov, Z. Wei, R. Heitz, A. Madhukar. *Appl. Phys. Lett.*, **75**, 85 (1999).
- [14] D. Leonard, K. Pond, P.M. Petroff. *Phys. Rev. B*, **50**, 11 687 (1994).
- [15] A. Polimeni, A. Patane, M. Cappizi, F. Martelli, L. Nazi, G. Salvani. *Phys. Rev. B*, **53**, R4213 (1996).
- [16] A. Patane, M.G. Alessi, F. Intonti, A. Polimeni, M. Capizzi, F. Martelli, L. Nasi, L. Lazzarini, G. Salviati, A. Bosacchi, S. Franchi. *J. Appl. Phys.*, **83**, 5529 (1998).
- [17] V.G. Dubrovskii, G.E. Cirlin, Yu.G. Musikhin, Yu.B. Samsonenko, A.A. Tonkikh, N.K. Polyakov, V.A. Egorov, A.F. Tsatsul'nikov, N.A. Krizhanovskaya, V.M. Ustinov, P. Werner. *J. Cryst. Growth*, **267**, 47 (2004).
- [18] V.G. Dubrovskii, G.E. Cirlin, V.M. Ustinov. *Phys. Status Solidi B*, **241**, R42 (2004).
- [19] A.V. Osipov, F. Schmitt, S.A. Kukushkin, P. Hess. *Appl. Surf. Sci.*, **188**, 156 (2002).
- [20] V.G. Dubrovskii, G.E. Cirlin, V.M. Ustinov. *Phys. Rev. B*, **68**, 075 409 (2003).
- [21] U. Perinetti, N. Akopian, Yu.B. Samsonenko, A.D. Bouravleuv, G.E. Cirlin, V. Zwiller. *Appl. Phys. Lett.*, **94**, 163 114 (2009).
- [22] V.G. Dubrovskii, N.V. Sibirev, X. Zhang, R.A. Suris. *Cryst. Growth Des.*, **10**, 3949 (2010).
- [23] X. Zhang, V.G. Dubrovskii, N.V. Sibirev, X. Ren. *Cryst. Growth Des.*, **11**, 5441 (2011).
- [24] V.G. Dubrovskii, V. Consonni, A. Trampert, L. Geelhaar, H. Riechert. *Phys. Rev. B*, **85**, 165 317 (2012).

*Редактор Т.А. Полянская*